AGU PUBLICATIONS

Space Weather

REVIEW ARTICLE
10.1002/2016SW001547

Special Section:
Reprise of 2001 Space Weather Monograph

Seismic imaging of the Sun's far hemisphere and its applications in space weather forecasting

Charles Lindsey[1] and Douglas Braun[1]

[1] NorthWest Research Associates, Boulder, Colorado, USA

Key Points:
- The Sun is filled with acoustic waves with periods ranging from about 2 to 8 min
- Observations of these waves allow us to make synoptic seismic maps of active regions in the Sun's far hemisphere
- These synoptic maps of the Sun's far hemisphere are a valuable resource for space weather forecasting

Correspondence to:
C. Lindsey,
clindsey@nwra.com

Citation:
Lindsey, C., and D. Braun (2017), Seismic imaging of the Sun's far hemisphere and its applications in space weather forecasting, *Space Weather*, *15*, 761–781, doi:10.1002/2016SW001547.

Received 6 OCT 2016
Accepted 11 FEB 2017
Accepted article online 17 FEB 2017
Published online 29 JUN 2017

Abstract The interior of the Sun is filled acoustic waves with periods of about 5 min. These waves, called "*p* modes," are understood to be excited by convection in a thin layer beneath the Sun's surface. The *p* modes cause seismic ripples, which we call "the solar oscillations." Helioseismic observatories use Doppler observations to map these oscillations, both spatially and temporally. The *p* modes propagate freely throughout the solar interior, reverberating between the near and far hemispheres. They also interact strongly with active regions at the surfaces of both hemispheres, carrying the signatures of said interactions with them. Computational analysis of the solar oscillations mapped in the Sun's near hemisphere, applying basic principles of wave optics to model the implied *p* modes propagating through the solar interior, gives us seismic maps of large active regions in the Sun's far hemisphere. These seismic maps are useful for space weather forecasting. For the past decade, NASA's twin STEREO spacecraft have given us full coverage of the Sun's far hemisphere in electromagnetic (EUV) radiation from the far side of Earth's orbit about the Sun. We are now approaching a decade during which the STEREO spacecraft will lose their farside vantage. There will occur significant periods from thence during which electromagnetic coverage of the Sun's far hemisphere will be incomplete or nil. Solar seismology will make it possible to continue our monitor of large active regions in the Sun's far hemisphere for the needs of space weather forecasters during these otherwise blind periods.

1. Introduction

Magnetic regions in the Sun's outer atmosphere exert major impacts on space weather in the near-Earth environment. Near-term impacts on Earth are predominantly due to magnetic regions in the Sun's *near* hemisphere. However, because the Sun rotates, magnetic regions in the far hemisphere cross into the near hemisphere with little warning—except for our ability to monitor the Sun's far hemisphere much as we do the near hemisphere. For the past several years NASA's twin STEREO spacecraft have been in positions to view the entirety of the far hemisphere from the far side of Earth's orbit about the Sun. The STEREO spacecraft are gradually drifting back to Earth's side of our orbit about the Sun and in a few years will lose their farside vantage. There will occur significant periods from thence during which electromagnetic coverage of the Sun's far hemisphere will be incomplete or nil.

Our helioseismic observatories offer an attractive resource for the continued monitor of the Sun's far hemisphere in periods during which electromagnetic observations of the Sun's far hemisphere will be unavailable or incomplete. We have developed algorithms capable of analyzing seismic observations of the Sun's near hemisphere to map large active regions in the Sun's far hemisphere. This offers a promising resource for the continued monitoring of the Sun's far hemisphere for the indefinite future.

This chapter will give a brief review of the basic principles of solar seismology, the history of their conceptual and observational development, and their adaptation as an opportune spin-off for synoptic mapping of active regions in the Sun's far hemisphere that can serve the practical needs of space weather forecasting. We will proceed then to illustrate how seismic monitoring of the Sun's far hemisphere works in practice. We will end the chapter with a summary of some of the major practical applications of far-hemispheric monitoring in space weather forecasting.

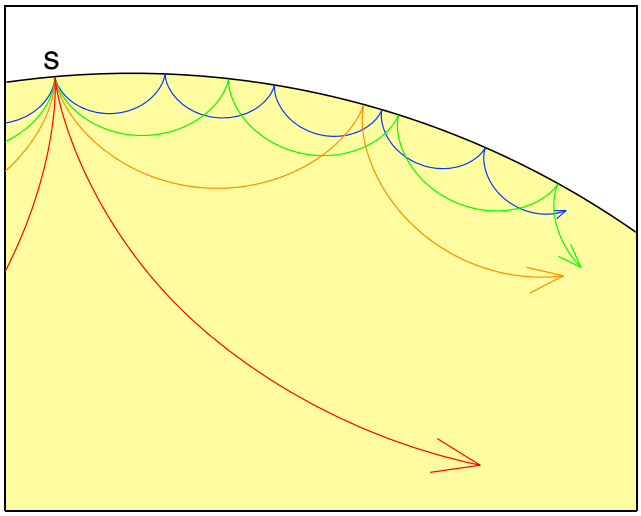

Figure 1. Unlike electromagnetic radiation in a vacuum, sound waves in the solar interior are continuously refracted, following curve paths that return them to the surface in distance usually much shorter than that of the straight-line trajectory tangent of the path at the source, *S*. Waves with periods around 5 min are specularly reflected at the surface. They continue for multiple skips beneath the surface before they eventually lose their coherence or decay.

2. Basic Principles of Farside Solar Seismology

The ability to monitor the Sun's far hemisphere by analyzing observations of seismic oscillations over its near hemisphere is a classical spin-off from a broad field of solar research called *helioseismology*. The acoustic waves of which the solar oscillations are a surface signature are understood to be excited almost entirely by convective motion in a narrow layer comprising just the outer few hundreds of kilometers of the Sun's convection zone. (The convection zone is understood to extend from about what we identify as the Sun's *surface* at its outer extreme, to a depth of about 0.3 solar radius, i.e., ~210,000 km, beneath said surface.) The particular *p* modes of use for monitoring the Sun's far hemisphere emanate downward from the outer convection zone, penetrating deep into the Sun's interior. But, unlike electromagnetic waves in a vacuum, acoustic waves in the solar interior are subject to strong refraction. They generally travel along upwardly curving "ray paths," (see Figure 1) most of them returning to the surface in less than a radian along the solar surface. Upon reaching the surface, they undergo a specular reflection back into the Sun's interior, retaining most of their coherence. From thence, they adhere closely to a continued ray path identical to the previous one, beginning anew from the point of reflection, proceeding the same direction as before beneath the great circle along the Sun's surface connecting the origin with the reflection point. By multiple such specular reflections, a vast swarm of *p*-mode waves excited by convection travel beneath a myriad of solar circumferences, reverberating between the Sun's near and far hemispheres multiple times before they eventually lose their coherence and decay.

The *p* modes obey basic principles very similar to those obeyed by electromagnetic waves, such as those we recognize as visible light. We are no better familiar with these principles than by virtue of the great variety optical techniques we have applied to visible light in our development of *remote sensing*. Our optical devices, typically based upon one or more lenses, sample electromagnetic disturbances in a given region, $\mathcal{P}$, the "pupil" of the device, over some surface, $\mathcal{S}$, containing $\mathcal{P}$, to image the source distribution of the seismic radiation (i.e., the *p* modes) understood to have brought these disturbances to $\mathcal{P}$ in $\mathcal{S}$ from a considerable distance. We can similarly use the solar oscillations observed at the *Sun's* surface to image the source distributions of said seismic radiation, again over domains a considerable distance from that over which the oscillations are observed.

With this background, we can state formally the basic undergoings that make seismic monitoring of the Sun's far hemisphere possible.

1. Convection in the extreme upper convection zone produces acoustic waves (*p* modes) with periods of several minutes that penetrate deep into the Sun's interior.
2. The *p* modes obey principles highly analogous to those from which electromagnetic optics benefit.
3. The *p* modes communicate between opposite hemispheres of the Sun, retaining their coherence from one to the other.
4. The *p* modes interact strongly with active regions when they encounter them at the Sun's surface and carry the signature of that interaction with them as they reflect back into the solar interior, retaining it from one hemisphere to the other.

5. The *p* modes make a clearly observable seismic signature where they encounter the Sun's surface, identified as "the solar oscillations." The component of this oscillatory signature in the Sun's near hemisphere is mapped in spatial and temporal detail by our helioseismic observatories.

The major difference between the familiar electromagnetic optics we use in the terrestrial environment and those applied to the signatures of acoustic waves observed at the Sun's surface is that the latter are essentially *computational*. Acoustic lenses are routinely used to image the sources of acoustic waves in the ocean, for example, just as electromagnetic lenses are used to image the sources of visible light in air or in a vacuum. It is not yet practical to submerge acoustic lenses into the Sun's interior. Nor can we submerge acoustically sensitive surfaces to map the acoustic images projected by any such optics. What we can rather do is to apply the disturbances we infer from the solar oscillations on the Sun's near surface to the surface of an appropriate *acoustic model* of the solar interior and *computationally simulate* the waves in the model interior to be associated therewith. And we can sample acoustic disturbances over any surface at any depth in a computer model of the solar interior to an extent we have not the technology to do in the Sun itself.

A great deal of our ability to monitor the Sun's far hemisphere by the foregoing faculties is owed to the development of helioseismology, an area of research that began in the 1960s whose primary theme has been the use of observations of solar oscillations at the Sun's surface, and our understanding of these as a manifestation of acoustic waves that inhabit the solar interior, to infer the thermal structure of the solar interior and its flows from surface to core. We will proceed with a brief historical review of this field and describe basic properties of the acoustic waves of which it is diagnostic.

2.1. Helioseismology

What we now call the solar oscillations were discovered independently by *Leighton et al.* [1962] and *Evans et al.* [1963], by observing temporal variations in Doppler shifts of photospheric lines over the Sun's surface. These oscillations, found to have periods ranging from about 2 to 8 min, were soon recognized as the surface signature of acoustic waves in the Sun's photosphere [*Noyes and Leighton*, 1963]. The waves of which the solar oscillations are a signature were eventually understood to be excited by convection a few hundreds of kilometers beneath the Sun's surface [*Stein et al.*, 2004], some of which penetrate hundreds of thousands of kilometers into the Sun's interior [*Ulrich*, 1970].

In applying the term "acoustic" to such waves, we must admit that the spectrum of the oscillations in question is far lower in frequency, by a factor of about 10^5, than the familiar acoustic spectrum to which our ears are sensitive. The applicability of acoustic in spite of this rather capitalizes on the waves of which the disturbances are a signature being "compressional" in the same sense as that which we call "sound," here on Earth. That is, the predominant restoring force acting on the disturbances of which the waves are comprised is that of gas pressure, and this acts against an inertia that is entailed in the mass density of the medium.

Ulrich [1970] introduced the idea of using the solar oscillations as a diagnostic of the Sun's interior structure. *Deubner* [1975] and *Rhodes et al.* [1977] developed this at length, as a diagnostic of both the thermal structure of the solar interior and of the dependence of differential rotation with depth. In the late 1980s and early 1990s, solar seismology began to develop along two significantly separate theoretical and observational lines, distinguishing between "global" and "local" helioseismology. Global helioseismology views the Sun as a collection of harmonic oscillators, capitalizing on highly accurate measurements of the frequencies of its myriad of normal modes to develop a model of its overall thermal structure. The normal mode frequencies also give us a credible model of how the solar interior rotates. Global diagnostics give us sharp discrimination in depth and some in latitude but none in longitude. It has given us maps of the solar interior rotation rate [*Rhodes et al.*, 1979], affirming that the Sun is a differentially rotating fluid. We understand that the equatorial interior rotates significantly faster than the poles, as it does at the surface, down to the base of the convection zone, that the region of fastest rotation is about 10,000 km beneath the equatorial photosphere, and beneath that the rotational angular velocity decreases. Global helioseismology also tells us the thermal structure of the solar interior [*Christensen-Dalsgaard et al.*, 1993], identifying the base of the convection zone at a radius of $\sim 0.7 R_\odot$ from Sun center. It also reveals a reversal of the sound speed gradient in the Sun's core, implying a high concentration of helium therein.

What is recognized as "local helioseismology" looks at the foregoing acoustic waves more from the perspective of optics, to focus on relatively compact *anomalies* in an otherwise nominal medium

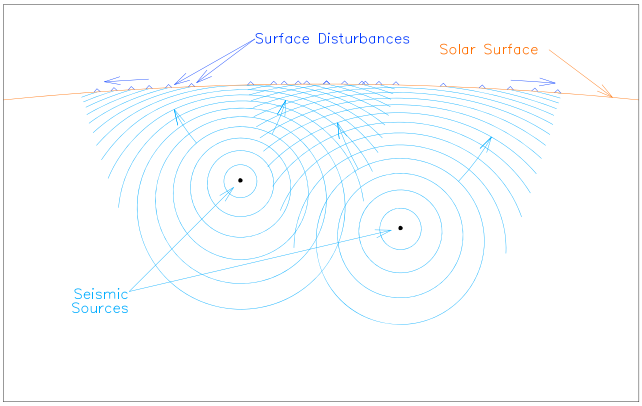

Figure 2. Wavefronts, represented here as expanding turquoise rings, emanate from seismic sources embedded in a model of the solar interior. Where these wavefronts break to the surface, they manifest outwardly propagating surface ripples beginning directly above respective sources and propagating outward along the surface therefrom. Curved trajectories terminated by arrow heads represent segments of the ray paths that characterize refraction in the solar medium (see Figure 1). Reproduced from *Lindsey et al.* [2011], courtesy of InTech (http://www.intechopen.com).

[*Braun et al.*, 1988; *Braun and Birch*, 2008]. It is this local perspective of solar seismology under which the ability to seismically image active regions in the far hemisphere has been developed [*Lindsey and Braun*, 1990; *Braun et al.*, 1992]. Active regions represent relatively localized anomalies in a solar environment that is otherwise highly uniform over any given layer in radial distance, i.e., very close to spherically symmetric.

2.2. Helioseismic Holography

The idea of adapting basic principles of wave optics to helioseismic observations as described in section 2 is called *computational helioseismic holography*. The basic concept was introduced by *Roddier* [1975] as a suggested means of imaging acoustic sources submerged beneath the solar photosphere. *Lindsey and Braun* [1990] proposed this as a means of imaging sunspots in the *far photosphere*, i.e., viewing them acoustically *through* the solar interior from the surface of the Sun's near hemisphere. Further developments are described by *Braun et al.* [1992], *Lindsey et al.* [1996], and *Lindsey and Braun* [1997] (relating seismic holography to the more recently introduced "time-distance helioseismology" of *Duvall et al.* [1993] and *Duvall et al.* [1996]) and further by *Chang et al.* [1997], *Braun et al.* [1998], *Chou* [2000], *Braun and Lindsey* [2000a, 2000b], *Braun and Lindsey* [2001], *Lindsey and Braun* [2000b], *Skartlien* [2001, 2002], and others.

Helioseismic holography is intended to take advantage of the fine *local discrimination* given to us by diffraction-limited optics. The local discrimination our eyesight gives us in the electromagnetic spectrum is a benefit of the preservation of *phase coherence* [*Zernike*, 1938; *van Cittert*, 1939] as light travels from its source to our eyes. A similar benefit is found in acoustic waves traveling through the solar interior and reflecting from the Sun's surface.

In its general form, helioseismic holography can be thought of as a development emerging from the following conceptual exercise in coherent wave optics [see *Lindsey and Braun*, 2000b]: We imagine an idealized acoustic model of the solar surface and its underlying interior with a few monopolar acoustic sources embedded therein. This is illustrated in Figure 2. Acoustic radiation emanating from these two sources is expressed in terms of an acoustic field, ψ, disturbances in which are represented as ring-like (in a planar slice, bubble like in three dimensions) wavefronts that expand outward, hence both upward and downward as time proceeds. Segmental samples of the upwardly curving ray paths (which are perpendicular to the wavefronts) are included in Figure 2, terminated by arrow heads to indicate the upwardly curving direction into which the wavefronts are propagating. The only observable manifestation of $\psi(\mathbf{r}, t)$ is the disturbances that appear at the surface, $\mathcal{S}_0$. These disturbances first appear at points on $\mathcal{S}_0$ directly above the sources from which they emanated and propagate from thence outward along $\mathcal{S}_0$. These surface ripples traveling across $\mathcal{S}_0$ are the essence captured by helioseismic observations in such a scenario.

We now consider a detailed *record*, ψ_0, of the surface value of ψ taken from the foregoing helioseismic observations over some domain, $\mathcal{R}$, in $\mathcal{S}_0$ for a duration of a few oscillatory periods. Formal computational acoustic holography, as prescribed by *Lindsey et al.* [2011], consists of the following composite operation:

1. Apply the surface disturbance, ψ_0, in some domain, $\mathcal{P} \in \mathcal{S}_0$, *in time reverse* to the surface, $\mathcal{S}_0$, of an *acoustic model* of the solar medium that itself is devoid of sources, absorbers, or other significant anomalies.
2. Allow the acoustic model to propagate the resulting disturbances backward into its interior.
3. Then, sample the regressed acoustic field in some domain within the model.

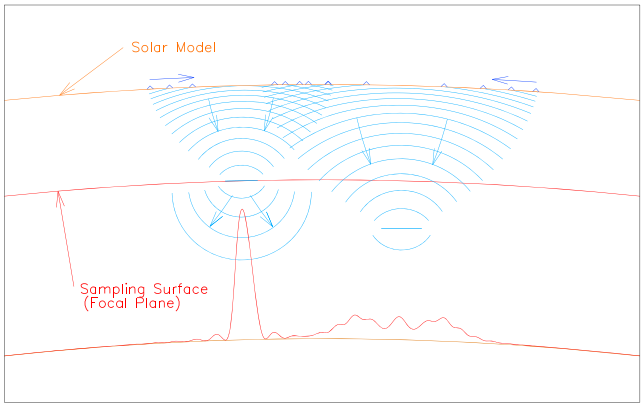

Figure 3. Coherent computational regression of the surface acoustic field into a computationally accessible model of the solar interior. A record, ψ_0, of the surface acoustic field is applied computationally to the model surface in time reverse to drive a disturbance that propagates backward into the model interior. This coherent acoustic egression, $H_+(\mathbf{r}, t)$ can be sampled anywhere in the model interior. We call the acoustic power, $|H_+(\mathbf{r}, t)|^2$, of this regressed acoustic field the "egression power" of ψ_0. This is averaged over time along a "sampling surface" (red) whose depth is the same as that of the leftward seismic source in Figure 3 and plotted radially beneath it (bottom of frame). Reproduced from *Lindsey et al.* [2011], courtesy of InTech (http://www.intechopen.com).

We call the time-reversed acoustic field, $H_+(\mathbf{r}, t)$, in the model the "coherent acoustic egression" of ψ_0. $H_+(\mathbf{r}, t)$ is a coherent reconstruction of a component of ψ that arrived at the solar surface, $\mathcal{S}_0$, with every apparent intention of egressing through it—hence the term "egression,"—from the interior of the medium, supposing that the medium provided somewhere on the other side of $\mathcal{S}_0$ for it to continue into—or, perhaps, the mechanism to simply absorb it. (The idealized acoustic model is supposed to register the signature we have identified as ψ_0, whereafter the wave that caused it then goes away—and does not come back some time later to complicate the interpretation of ψ_0 as to its supposed source.)

Figure 3 illustrates steps 2 and 3, above, for a sampling domain on a surface, $\mathcal{S}_z$, of constant depth, z, radially beneath $\mathcal{S}_0$. In fact, Figure 3 attempts to convey diagramatically significant respects in which the regressed acoustic field differs from the actuality diagrammed in Figure 2. Approaching the source locations from above, the regressed acoustic field does not fully condense into the point sources of its counterparts in Figure 3. This is an essential consequence of the acoustic model in Figure 3 not including point absorbers to play the time reverse role of the point sources in Figure 2. Rather than disappearing back into their sources, the waves in the regressed acoustic field continue downward through their respective source layers and into the underlying model interior. This behavior is entirely similar to that which applies in familiar lense optics.

$H_+(\mathbf{r}, t)$ nevertheless condenses into conspicuously compact kernels at the locations of the respective sources. The kernel representing the leftward source in Figure 3 is clear in a plot of $|H_+(\mathbf{r}, t)|^2$ along a sampling surface at the depth of said source (see left side of the plot at the bottom of Figure 3). For the rightward source, which lies deeper than the sampling surface (right side of egression-power plot), the egression-power signature remains extant but is out of focus, hence diffuse—as it would similarly be for a source *above* the sampling surface.

The actual degree to which H_+ in fact succeeds in emulating the time reverse of ψ in practice is contingent upon several factors: These begin with (1) the limited completeness of the foregoing surface application, in terms of the limited pupil $\mathcal{P}$ over which ψ_0 is applied (in time reverse) to $\mathcal{S}_0$, and in the ability of the observations to fully characterize all aspects of the surface disturbance and (2) any loss in phase coherence retained by the wave as it propagates through the medium from source to pupil.

Incompleteness of the surface application has an analogy in electromagnetic optics in *diffraction* due to an entrance pupil that is invariably limited. This is customarily expressed in terms of smearing of the image [*Born and Wolf*, 1975b]. Loss of phase coherence is analogous to the quality lost by electromagnetic radiation to some degree when it encounters optical anomalies, such as in atmospheric turbulence or clouds [*Born and Wolf*, 1975a]. This appears to be negligible for acoustic waves at depths exceeding a few hundreds of kilometers into the Sun's interior. In the acoustic context, the vast bulk of the solar interior appears to be of a remarkably high optical quality.

2.3. Seismic Holography Applied to the Sun's Far Hemisphere

Geometrically speaking, seismic holography of the Sun's far hemisphere can be considered a straightforward extension of the simple examples illustrated by Figures 2 and 3 if the sampling surface in Figure 3 is distended first downward, past the center of the Sun, and from thence all the way to the surface of the far hemisphere.

However, when this is done, the upward curvature of the ray paths, which is somewhat subtle for the short ray path segments in Figures 2 and 3, becomes important in ways we have yet to confront. For mapping the Sun's far hemisphere, curvature of the ray paths becomes critical, as does the curvature inherent in any spherically symmetric medium.

2.3.1. Acoustic Refraction

Curvature of ray paths due to refraction (see Figure 1) is fairly familiar on Earth in mirages seen above a flat expanse such as the Mojave Desert in June, due to excess heating of air a few feet above the sand. Said heating reduces the density of the medium and its refractive index, making the speed of light through that air slightly greater than at a greater height. This causes a ray path nominally parallel to flat ground to curve upward, as prescribed by Snell's law: In the familiar instance of a vertically stratified medium in a plane-parallel geometry, Snell's law can be expressed by

$$\sin\theta = Kc, \tag{1}$$

where θ signifies the angle of the tangent to the ray path, Γ, at a given point, P, from directly vertical; c signifies the speed of light in the medium at the height of P; and K is a constant that identifies the ray path under consideration. (For example, if the value of c at P is c_0, and the ray path desired passes through P at an angle θ_0 from vertical, then $K = \sin\theta_0/c_0$ all along that ray path.) When c decreases with height, $\sin\theta$ does likewise, as does θ itself; hence, the ray path becomes more vertical with increasing height and therefore curves upward.

In the terrestrial atmosphere, the variation in c is not very large, and it is only because of the high acuity of our eyes that we can resolve mirages. For the species of acoustic waves in the solar interior that most readily communicate between opposing hemispheres in the solar interior the effects of refraction are anything but subtle: These waves must travel a long distance from one surface encounter to the next, penetrating deep beneath the surface between encounters. The practical model to represent this behavior replaces the flat expanse in the Mojave Desert with a spherically symmetric medium that approximates the sound speed, c, as a function of r, the radial distance of the reference point, P, from the center of the Sun.

In such a spherically symmetric medium, Snell's law transforms to

$$r\sin\theta = Kc, \tag{2}$$

where θ is now the angle between Γ and the local radial direction at P and r is the radial distance of P from the center of spherical symmetry, i.e., the center of the solar interior. As in the plane-parallel case, a constant sound speed prescribes a straight ray path, while a sound speed that decreases with increasing r prescribes one that curves upward. Any ray path, Γ, that is aimed downward from the Sun's surface but not directly toward the Sun's center, i.e., $\sin\theta_0 > 0$, curves progressively farther away from the radially downward direction with increasing depth, eventually reaching a minimum radial distance,

$$r_{\min} = Kc, \tag{3}$$

i.e., where $\sin\theta$ has become unity. From this point it continues its upward curvature, eventually returning to the surface. In this geometry, K all along the optical path, Γ, is fixed at its surface value,

$$K = \frac{R_\odot \sin\theta_0}{c_0}, \tag{4}$$

with θ_0 the nonzero angle of the ray path from the radial at the Sun's surface and c_0 is the speed of sound thereat.

The solar interior has a strong negative temperature gradient with increasing radial distance, r, extending from its core to its surface. The speed of sound in the Sun's core is understood to drop from about 500 km/s in its core to about 8 km/s at its surface. Figure 4 shows a sample of ray paths, and associated wavefronts, for the family of waves that propagate from a focus in the far hemisphere to points in the near hemisphere in two skips, with a specular reflection halfway in between. Consecutive wavefronts are separated by 5 min. The total one-way travel time from the source in the far hemisphere to the surface of the near hemisphere is in the range (3.5 ± 0.25) h.

2.3.2. The Specular Reflections and Multiple-Skip Seismology

The diagram in Figure 4 illustrates both a major difficulty imposed by refraction of waves due to the strong sound speed gradient in the solar interior and how this difficulty can be alleviated by taking advantage of the

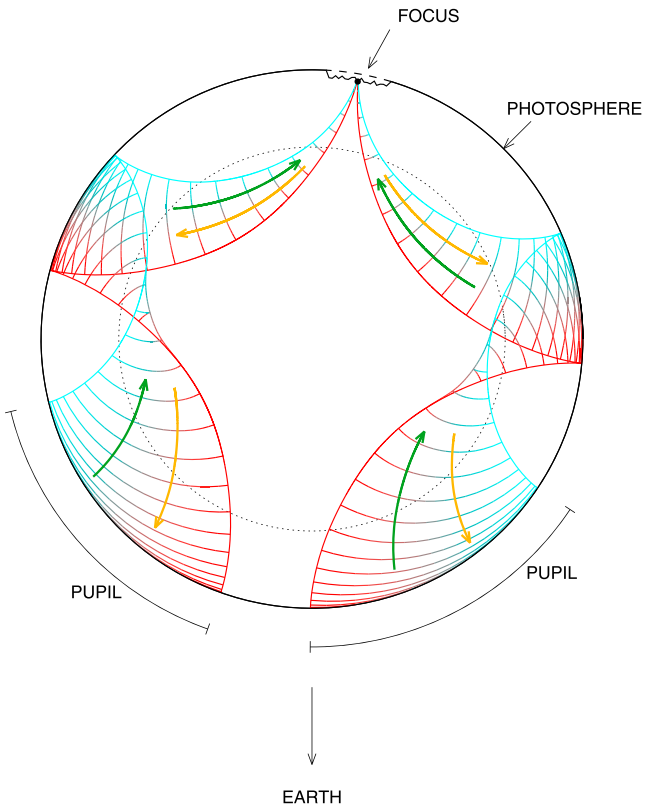

Figure 4. Diagram of wavefronts (loci fading from red to turquoise) and ray paths (solid red, solid turquoise, and green and yellow arrows) representing a cross section of waves traveling to and from a "focus" (top) and reflecting from the Sun's surface once during their travel between the far hemisphere (top) and the near hemisphere (bottom). Reproduced from *Lindsey et al.* [2011], courtesy of InTech (http://www.intechopen.com).

specular reflections that occur when these waves encounter the Sun's surface. The curvatures of the ray paths due to refraction are seen to range from approximately $(1.0-1.5)/R_\odot$ from those with the longest skip distance to those with the shortest. This radically shortens the distance traveled by waves emanating from the surface along ray paths that begin with angles, θ_0, more than a degree from vertically downward, in only a single skip. The tangents to the ray paths at their surfaces range from 0.64° for the ones that penetrate deepest (red) to 2.9° for the shallowest (turquoise). If the sound speed, c, in the solar interior were constant, all of the ray paths emanating from the focus in Figure 4 would proceed straight along said tangents from their origin at said focus to arrive in the near hemisphere within ~6° of the antipode of the focus in the far hemisphere. Because of refraction, none of these ray paths reach the near hemisphere in a single skip. However, by continuing a single additional skip from their first surface encounters, after a specular reflection, they all arrive into the opposing hemisphere, within 75° of the antipode of the focus, which is within the practical observing range of helioseismic observations from directly over said antipode.

In point of fact, there actually is a family of waves that travels directly from the far hemisphere to the near hemisphere in a single skip. These are confined to surface tangent angles, θ_0, within 0.33° of vertically downward. This narrow cone comprises a much smaller fraction of the acoustic spectrum than that which encompasses angles up to 2.9° but requires the additional skip. The additional skip, then, opens approximately $(2.9/0.33)^2 = 75$ times the spatial acoustic spectrum inhabited by waves that propagate from the focus to the near hemisphere in only a single skip. This results in seismic images with proportionately greater spatial resolution, ΔA, (in area) and "statistical weight" (W) for a given integration time of the seismic signature: We will return to this consideration in sections 3.1 and 3.2.

2.3.3. Acoustic Scattering and Phase Correlation Seismology

Up to now, we have treated the objects of seismic monitoring as simple acoustic sources, which can be mapped simply by integrating the acoustic power, of the regressed acoustic field integrated over some period of time

$$P(\mathbf{r}) = \int \mathrm{d}t\, |H_+(\mathbf{r},\, t)|^2. \tag{5}$$

This is what is plotted in red at the bottom of Figure 3, and this form of the diagnostic is called "acoustic power holography." Acoustic power holography is also sensitive to acoustic absorbers, showing them in silhouette. Active regions are known to be strong absorbers of obliquely incident acoustic waves [*Braun et al.*, 1988; *Braun and Birch*, 2008] as they reflect them back into the solar interior, i.e., waves with skip distances of a few tens of Mm. Inconveniently, this strong absorption appears to abate for waves approaching normal (locally vertical) incidence [*Lindsey and Braun*, 2000a], i.e., those with skip distances sufficient to take them to the opposing hemisphere within two skips. At this writing, the details of this behavior are only well enough understood for us to say that two-skip egression-power mapping of the Sun's far hemisphere is inadequate to realistically reveal active regions that are clearly visible by other means. Their signatures in egression power are like that of a white cat in a white room. (We are indepted to former summer student Mark Fagan for this apt analogy.) They are invisible.

Active regions are, nevertheless, strong *scatterers* of acoustic waves reflecting back into the solar interior from their photospheres, whether the incidence is normal or oblique. Their primary effect of benefit to seismic monitoring of the Sun's far hemisphere is to locally shift the *phase* of the reflection by a fraction of a radian, with respect to that of the quiet photosphere. This shift expedites the arrival of the echo back into the near hemisphere by a few seconds. A convenient physical model for this effect supposes that the active region photosphere is physically *depressed* some tens of kilometers by magnetic forces so that an upcoming wave encounters the reflecting layer a few seconds *before* its counterpart impinging upward into the quiet Sun. This "acoustic Wilson depression" appears to be an extension of the classical Wilson depression observed in sunspot umbrae [*Lindsey et al.*, 2010]. The standard diagnostic of the phase shift attached to such a perturbation involves a comparison between acoustic radiation impinging *into* the focus and its outcoming *echo*. The echo is the egression, H_+, introduced above (see yellow arrows in Figure 4). The amplitude of acoustic radiation coherently converging into the focus—we call this the "coherent acoustic ingression" and denote it by "H_-"—is the time-forward analogy of H_+. It is the surface disturbance, ψ_0, in the near hemisphere propagated into the acoustic model *forward* in time (see green arrows in Figure 4), as opposed to the time reverse application of ψ_0 prescribed at the surface to derive the acoustic egression. The basic phase relationship between the acoustic radiation, H_-, impinging into the focus and its *outcoming echo* is to be found in the statistical cross correlation,

$$C(\mathbf{r}, \tau) = \int \mathrm{d}t\, H_-(\mathbf{r},\, t) H_+(\mathbf{r}, t + \tau), \tag{6}$$

between H_- and H_+. The phase shift between H_- and H_+ can be expressed by integrating the Fourier transform, $\hat{C}$, of C, over the positive half of its frequency spectrum:

$$\phi(\mathbf{r}) \equiv \arg\left(\int_0^\infty \mathrm{d}\omega\, \hat{C}(\mathbf{r}, \omega)\right). \tag{7}$$

3. Farside Solar Seismology in Practice

The first seismic maps of the Sun's far hemisphere were published by *Lindsey and Braun* [2000a] [see also *Braun and Lindsey*, 2001] at the turn of the 21st century. These were computed from helioseismic observations by the Michelson-Doppler Interferometer (MDI) [*Scherrer et al.*, 1995] aboard the spaceborne Solar Heliospheric Observatory (SOHO). Since early 2001, Stanford's Solar Oscillations Investigation (SOI), the National Solar Observatory's Global Oscillations Network Group, and Stanford's Joint Science Operations Center (JSOC) for the Solar Dynamics Observatory (SDO) have maintained a continuous program of twice daily synoptic seismic maps of the Sun's far hemisphere [*González Hernández et al.*, 2007, 2009].

Over the 15 years since this synoptic mapping has begun, as the quality of the helioseismic observations has improved, the seismic maps have also improved. Other complementary diagnostics for seismic mapping of active regions in the far hemisphere have also been successfully opened: *Hartlep et al.* [2008] and *Ilonidis et al.* [2009] have developed a successful seismic monitor based on helioseismic *tomography* to map active regions

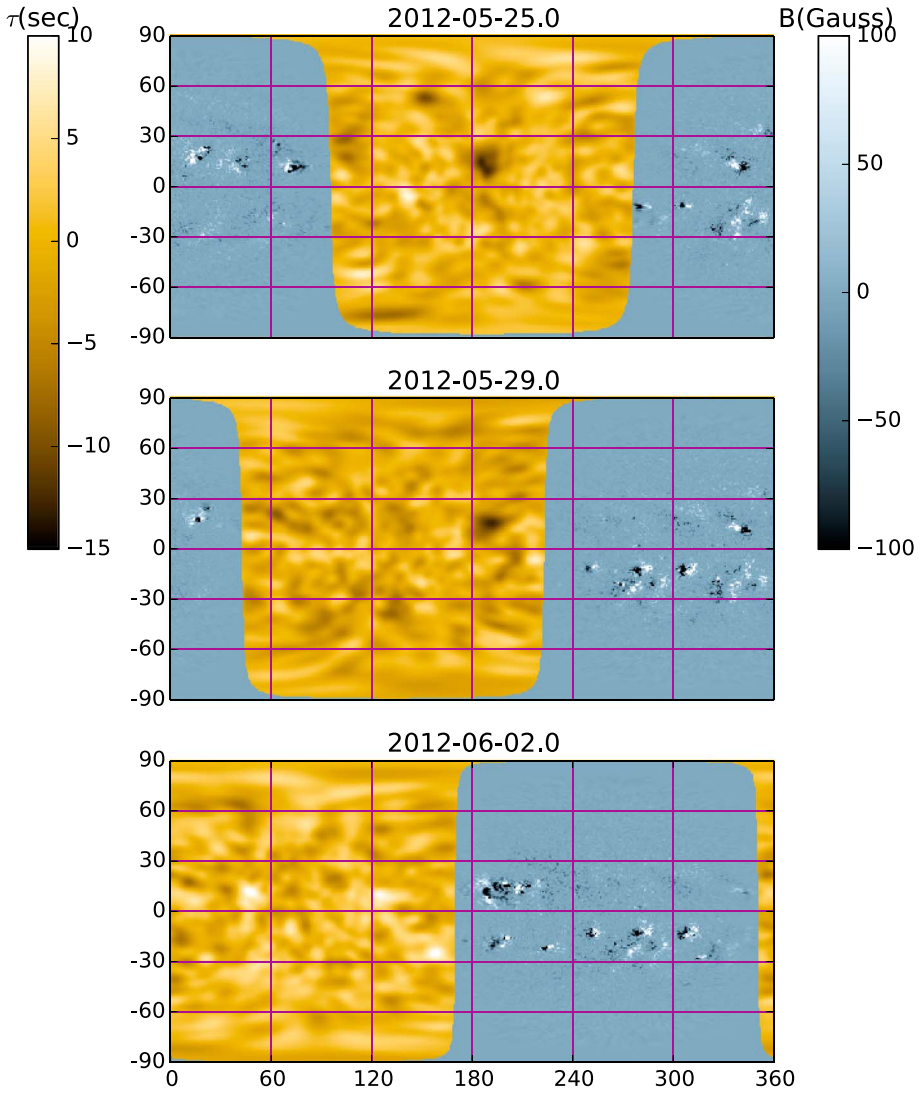

Figure 5. Composite maps of the Sun's far hemisphere (amber) and the line-of-sight magnetic field (blue gray) show NOAA AR 11498 at (190°W, 12°S) crossing (top) central meridian in the far hemisphere (amber) approaching the (middle) east limb (amber region moving leftward with respect to [190°W, 12°S]), and (bottom) having passed into the near hemisphere (blue gray), at which time it received the foregoing NOAA designation. The phase correlation signature is rendered in terms of the travel time perturbation, τ, carried by the echo from the magnetic photosphere in the far hemisphere as compared with the quiet Sun.

in the Sun's far hemisphere. Tomography capitalizes on the predominantly *specular* quality of reflections from relatively large, smooth distributions of magnetic flux. Reflections from more compact anomalies have significant nonspecular components. Holography capitalizes on the finer spatial resolution attainable by taking an account of these nonspecular components.

For a description of how farside seismology works in practice, we will focus on the synoptic seismic maps presently being published by the Stanford's SDO JSOC. These maps are publicly accessible through http://jsoc.stanford.edu/data/farside and are archived back to May of 2010 (about three months after the SDO was launched). The Stanford farside seismic monitor analyzes 31 h time series of Helioseismic Magnetic Imager (HMI) Doppler observations to produce twice daily travel time maps of the Sun's far hemisphere, each representing seismic cross correlations over a 24 h period. (The reason for the 31 h time series is the approximately 3.5 h acoustic travel time from near hemisphere to far hemisphere and the same for the returning echo. The period over which there is an actual correlation between $H_+(\mathbf{r}, t)$ and $H_-(\mathbf{r}, t)$ is reduced by the 7 h round trip. Each farside map then represents a correlation over a duration of $31-7 = 24$ h.) Figure 5 shows samples of the

standard 24 h farside seismic maps over the period 25 May 2012 (top) to 2 June 2012 (bottom). NOAA AR 11498 is seen at (190°W, 12°S), crossing the farside meridian (top), approaching the east limb (middle), and rotating into direct view (bottom) in the near hemisphere. In these renderings, the phase shift prescribed by equation ((7)) is expressed as a "travel time perturbation," τ, of the approximately 7 h round trip travel time required for acoustic waves to complete the circuit diagrammed in Figure 4

$$\tau \equiv \frac{\phi}{\omega_0} = \frac{\phi T_0}{2\pi}, \tag{8}$$

where T_0 is taken to be 5 min and it is understood that $\omega_0 = 2\pi/T_0$. The phase perturbation imposed by NOAA AR 11498 is equivalent to a reduction of up to ~12 s enjoyed by the echo returning from AR 11498 in the ~7 h round trip from the near hemisphere to the far hemisphere and back.

3.1. The Spatial Resolution of Farside Seismic Holography

The spatial resolution for the wave configuration in Figure 4 is most directly expressed by its electromagnetic analogy, i.e., the Abbe diffraction limit

$$\Delta s = 1.22\frac{\lambda_0}{2\sin\theta_0} = \frac{0.61c_0}{\nu_0\sin\theta_0} = \frac{0.61c_0T_0}{\sin\theta_0}, \tag{9}$$

where ν_0 is the temporal frequency of the seismic radiation; $T_0 \equiv 1/\nu_0$ is its temporal period, which we take to be 5 min, as it is in Figure 4; λ_0 is the wavelength, c_0T_0, approaching the surface; and we call θ_0 the "opening angle" of the optical configuration so represented. With $\theta_0 = 2.9°$, then, Δs works out to 10° of arc over the Sun's surface, to represent the family of waves that suffer a single specular reflection to reach the near hemisphere in two skips. For the family of waves that reach the near hemisphere in only a single skip, i.e., $\theta = 0.33°$, the diffraction limit explodes to 87°. This only marginally resolves the entire far hemisphere into more than a single region and is far from resolving the largest active regions. In summary, then, the facility of acoustically viewing the Sun's far hemisphere through at least one specular reflection is crucial to practical seismic monitoring of the Sun's far hemisphere out to anything approaching the antipode of disk center.

3.2. The Sensitivity of Farside Seismic Holography

Notwithstanding the adaptability of the most basic principles of optics in the electromagnetic spectrum, seismic monitoring of the Sun's far hemisphere is encumbered by fundamental limitations that make it far less sensitive than electromagnetic monitoring. This is mostly because of the vastly lower spectral bandwidth to which helioseismic observations are confined. The fundamental limitation in sensitivity is due to the limited statistical weight, W, introduced at the end of section 2.3.2, attached to a record of random noise over a limited spectral bandwidth, $\Delta\nu$, for a limited time, Δt. Table 1 shows a comparison of key temporal and spatial parameters contributing to W in a 1 ms electromagnetic snapshot by SDO/HMI light and a 1 day seismic integration.

For the seismic signature representing a single element of spatial resolution, we define W by

$$W \equiv \Delta\nu\Delta t. \tag{10}$$

Helioseismologists often call the uncertainty in a seismic signature imposed by this limit "realization noise." In the case of the phase, ϕ, of a cross correlation such as that expressed by equation ((7)), the realization uncertainty is

$$\Delta\phi \equiv \frac{1}{\sqrt{W}}, \tag{11}$$

in radians, which translates to an uncertainty in the travel time perturbation, τ, of

$$\Delta\tau = \frac{\Delta\phi}{\omega_0\sqrt{W}} = \frac{\Delta\phi}{2\pi\nu_0\sqrt{W}} = \frac{\Delta\phi T_0}{2\pi\sqrt{W}} \approx 1\text{s}. \tag{12}$$

The seismic signature of NOAA AR 11498 in Figure 5 appears to inhabit an area of ~$(10°)^2$, approximately the diffraction limit quantified in section 3.1, above. By its appearance in Figure 5, this signature has a signal-to-noise ratio of roughly 10.

Table 1. Comparative Electromagnetic and Seismic Parameters

Characteristic Parameter	Electromagnetic (Visible)	Helioseismic
ν_0	5×10^{14} Hz	3.3 mHz
$\Delta\nu$	5×10^{10} Hz	2 mHz
Δt	1 ms	1 day
W	5×10^{7}	1728
Δs	$(370\ \text{km})^2$	$(120\ \text{Mm})^2$

To get a preliminary idea of the overwhelming advantage that electromagnetic imaging has over seismic, it is instructive, though far from a complete analysis, to start with a comparison of W for visible electromagnetic radiation imaged by HMI with the same for seismic signatures. Table 1 lists appropriate electromagnetic values to accommodate this

$$\frac{W(\text{electromagnetic})}{W(\text{seismic})} = \frac{(5 \times 10^7/370^2)}{(1728/120,000^2)} \approx 1.7 \times 10^{10}, \tag{13}$$

in which we are now including an account for the much finer spatial resolution instruments such as SDO/HMI and SDO/AIA give us in the visible electromagnetic spectrum.

In fact, realistic statistical weights for visible and UV electromagnetic intensities emanating from the Sun in the visible and UV spectra, while far greater than for seismic images, are nothing like those for the phase shifts that characterize seismic realization noise. This is, firstly, because photons are quantized. The quantum-electromagnetic analogy to equation ((11)) is

$$\frac{\Delta I_\nu}{I_\nu} = \frac{1}{\sqrt{W(\text{quantum})}}, \tag{14}$$

where ΔI_ν represents the photon-statistical noise in the intensity, I_ν, and

$$W(\text{quantum}) \equiv \frac{2W}{e^{h\nu/kT} - 1} \tag{15}$$

now represents simply the expectation number of photons emanating from a black body of temperature T during the interval dt into the solid angle spanned by the imager's angular resolution, as prescribed by its aperture. Already in the visible spectrum, the factor $2/(e^{h\nu/kT} - 1)$ is only 0.03.

In the EUV spectrum, which is where solar activity is by far the most conspicuous—and is, accordingly, what really matters to space weather—it is most convenient to express signal-to-noise ratio in terms of simply the number of photons, N_ν, detected as follows:

$$\frac{\Delta I_\nu}{I_\nu} = \frac{\Delta N_\nu}{N_\nu} = \frac{1}{\sqrt{N_\nu}}. \tag{16}$$

In fact, electromagnetic observations are encumbered by noise sources that well exceed even those prescribed by photon statistics, as a result of fine structure variations in the magnetic flux distribution in the quiet Sun. We nevertheless find that the mean EUV intensities of strong active regions averaged are typically a few hundred times their mean RMS variation in the quiet Sun.

3.2.1. Comparative Applications in the Sun's Near Hemisphere

A great deal of our understanding of the farside seismic maps comes from comparative seismic imaging of active regions in the Sun's near hemisphere. These mappings benefit from shorter skip distances, hence greater opening angles, θ_0, giving us much finer spatial resolution, and can therefore discriminate the seismic signatures of different parts of an active region. Figure 6 shows seismic, visible light (continuum intensity and line-of-sight magnetic field) and EUV images of NOAA AR 11158 in the near hemisphere. One of the remarkable findings shown by nearside images, long before the first farside images were accomplished, was that, notwithstanding the far stronger magnetic fields of sunspots, the predominant component of the seismic signature of an active region is manifested invariably by the *plage surrounding* the sunspots, not the sunspots themselves. Our rough understanding of this is that the seismic signature can be roughly thought of as a measure of the photospheric depression of the active region due to Lorentz forces. While a strong magnetic field produces a deeper photospheric depression, the depth of the depression rapidly saturates with increasing magnetic pressure ($B^2/(8\pi)$), because of an approximately exponential increase in opposing gas pressure with depth. So at least in terms of acoustic indications, the sunspot umbra is depressed not so very much further than the magnetically weaker plage. The latter, then, predominates the overall acoustic signature simply

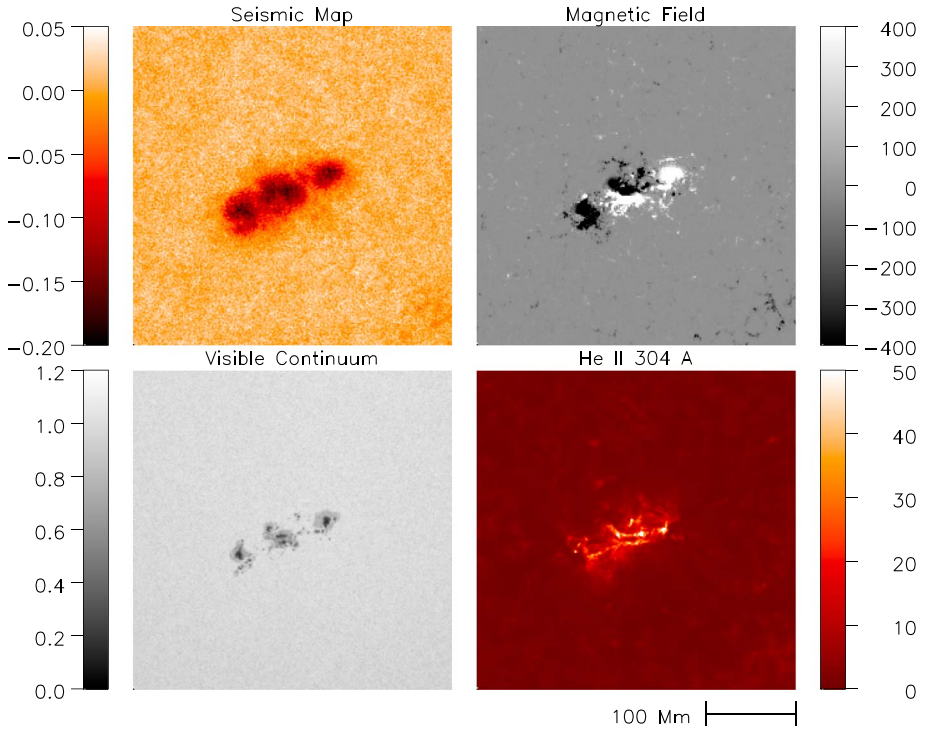

Figure 6. (top left) Seismic map of NOAA AR 11158 in the Sun's near hemisphere is shown at 15 February 2011 concurrently and cospatially with (bottom left) a visible continuum intensity map, (top right) a line-of-sight magnetic map, and (bottom right) a He II 304 Å intensity map.

because it inhabits many times the area of the sunspots. Indeed, it was recognition of this by *Braun and Lindsey* [2000b] that made the strong case to *Lindsey and Braun* [2000a] that active regions in the Sun's far hemisphere ought to be clearly visible in seismic maps of the far hemisphere while prospects for detecting just sunspots were marginal.

Another feature that is evident from Figure 6 is that seismic signatures of active regions tend to reflect the magnetic morphology of the active region much more closely than the source distribution of excess UV radiation emanating from the active region chromosphere and transition region. This is roughly consistent with the model, briefly mentioned above, that even plages are magnetically depressed, as least in terms of the depth at which upcoming acoustic waves are effectively reflected back into the solar interior. This is certain to be a radical oversimplification of a reality that involves the subtleties of coupling between fast and slow modes [*Cally*, 2000; *Cally and Bogdan*, 1997; *Schunker et al.*, 2008; *Spruit and Bogdan*, 1992; *Lindsey et al.*, 2010]. This could someday be clarified by stereo observations of plages in visible light from spaceborne platforms with differing vantages in heliocentric orbit. In the mean time, the simple model of a magnetically depressed plage photosphere appears to be useful for at least some purposes.

Greater seismic sensitivity can be attained, if at the expense of temporal resolution, by averaging the helioseismic signature over several days. For a considerable domain of purposes, the sensitivity gained by integrating the seismic signature for 5 days more than makes up for the loss in temporal resolution. Five day cumulations of 24 h integrations increase the number of active regions that can be clearly recognized transiting the far hemisphere from a few dozen in a solar cycle to several hundreds. This radical increase is because of the demographics of active region strengths rather than because of some kind of statistical magic. It is simply because the number of active regions exceeding a given magnetic flux, Φ, for example, increases so rapidly as Φ decreases.

But there is another feature of solar activity that further justifies the sacrifice of temporal resolution: If magnetic flux that has emerged into the photosphere could disappear anything like as suddenly as it can emerge, then the 5 day cumulations would be open to the liability of showing a signature when none was extant. In fact, this happens rarely or never. Once a large intrusion of magnetic flux has emerged into the photosphere,

however, suddenly, it does not appear to be in the general character of solar magneto-convection then to retract it, eject it, nor otherwise to disappear it except through predominantly diffusive processes that operate over a period of days or weeks [*Wang et al.*, 1991, 1994]. Moreover, it appears that, to the moderately trained eye, the 5 day cumulations are not very much less sensitive to rapidly emerging flux than the individual 1 day integrations. This is consistent with the consideration that the 1 day "snapshots" for any day can in fact be algebraically recovered from the series of 5 day cumulations.

In summary, then, for space weather forecasting purposes, the 5 day cumulations are very useful, notwithstanding a formal sacrifice in temporal resolution. These, then, will be the focus of the next section.

4. Applications of Farside Solar Seismology in Space Weather Research and Forecasting

Applications of monitoring of the Sun's far hemisphere to space weather research and forecasting are already many and appear to be rapidly growing. Before we elaborate on these we note that monitoring of the Sun's far hemisphere, while useful for the task of forecasting the appearance of active regions in the Sun's near hemisphere, is not, of itself, a forecasting facility. It remotely senses active regions in the far hemisphere at the time when the waves whose signatures it subsequently observes encounter them in the far hemisphere. So like other familiar sensing instruments (thermometers, barometers, wind vanes, etc.), it renders characterizations of its subjects in the recent past, not the future. Forecasting is something that remains to be done when it has delivered its product, and the success of this is contingent upon the ability of the subject to change unpredictably in the interim. With this in mind, we briefly describe two promising aspects of forecasting applications of seismic monitoring of the Sun's far hemisphere presently under development.

4.1. The Relationship Between Seismic Signatures and UV Irradiance

Generally, the earliest known space weather manifestation to be anticipated by a strong helioseismic signature in the Sun's far hemisphere is the effect that the associated active region will have on UV irradiance at Earth. Realistic forecasting of UV and EUV irradiance on Earth is crucial to projecting conditions in the Earth's ionosphere, thermosphere, and exosphere. Excess UV and EUV emission from the Sun inflates the Earth's exosphere, increasing drag on spacecraft—and space debris—in low Earth orbit by up to about an order of magnitude and causing their orbital elements to drift accordingly. Forecasting variations in the solar UV and EUV irradiance is therefore useful for projections of the orbital elements of spacecraft and tens of thousands of individual items of space debris through periods during which observations of these are forestalled by poor weather. We understand, for example, that NASA moves the International Space Station approximately once per month on the average to avoid a prospective collision with one or more pieces of space junk.

Figures 7 and 8 illustrate the relationship between seismic signatures of active regions in the Sun's far hemisphere and subsequent variations in UV and EUV irradiance. Figure 7 shows seismic signatures designated "FS-103" and "FS-101" in the Stanford JSOC's composite map of the Sun of 5 November 2014. Figure 8 shows HMI (top row) and AIA (bottom row) images of the Sun 12 days later, on 17 November 2014, when both FS-101 and 103 appear in the near hemisphere. At this point, NOAA has designated FS-101 as two adjoining active regions, ARs 12208 and 12207, and, a few days after, FS-103 as adjoining active regions 12214, 12209, and 12213. As indicated by the UV images, the active regions encompassed by FS-101 and FS-103 account for the preponderance of the excess UV and EUV radiation emanating from the Sun 12 days after their appearance in the far hemisphere.

In fact, Figure 8 somewhat understates the prospective urgency to be aware of active regions such as those shown in Figure 7: Because excess EUV emission emanates largely from heated gas that is relatively optically thin, it tends to appear bright from Earth vantage very soon after it crosses the eastern limb, i.e., long before it becomes likely that a coronal mass ejection (CME) from the region or ejecta from a flare is likely to hit Earth. Without the farside monitor, regions like FS-101 and 103 can gestate unseen for up to 2 weeks before appearing unexpectedly at the eastern limb just hours before giving rise to a sudden, unwelcome boost to the EUV irradiance at Earth. In summary, the farside monitor can extend our warning of large, fully developed active region approaching the Sun's eastern limb from about a day to possibly nearly 2 weeks, depending on when and where in the far hemisphere the newly emerged flux breaks the surface. A study by *Fontenla et al.* [2009]

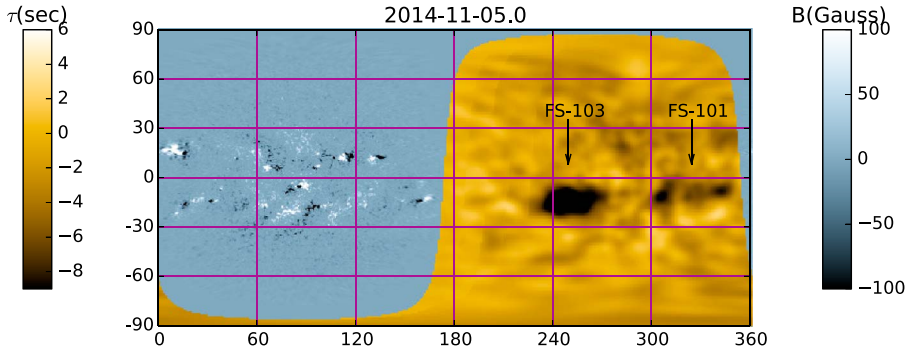

Figure 7. Composite seismic (amber) and magnetic (blue gray) map of the far and near hemispheres of the Sun in longitude (horizontal) and latitude (vertical) on 5 November 2014, a time of intense solar activity in the far hemisphere. Signatures of large active regions in the Southern Hemisphere are designated FS-103, at Carrington longitude 250° and FS-101 at 345°.

confirms a prompt improvement in a solar EUV irradiance forecast by including consideration of the seismic signature of newly emerged magnetic flux in the Sun's far hemisphere. This has yet to be implemented on a synoptic basis but is encouraging.

Work by *Liewer et al.* [2012, 2014] to calibrate seismic signatures with their EUV intensities has benefited from STEREO observations of the far hemisphere concurrent with the seismic maps. In a study of some 22 seismic signatures recognized by Stanford's Large Active Region Discriminator in early 2011 and early 2012, they found a high spatial correlation of these with regions of excess EUV (He II 304 Å) intensity, with no false alarms. However, they also identified a similar number of regions with conspicuous, if on-the-average somewhat weaker, EUV excesses that elicited no seismic signature at all or one that was insignificant. This has to be expected

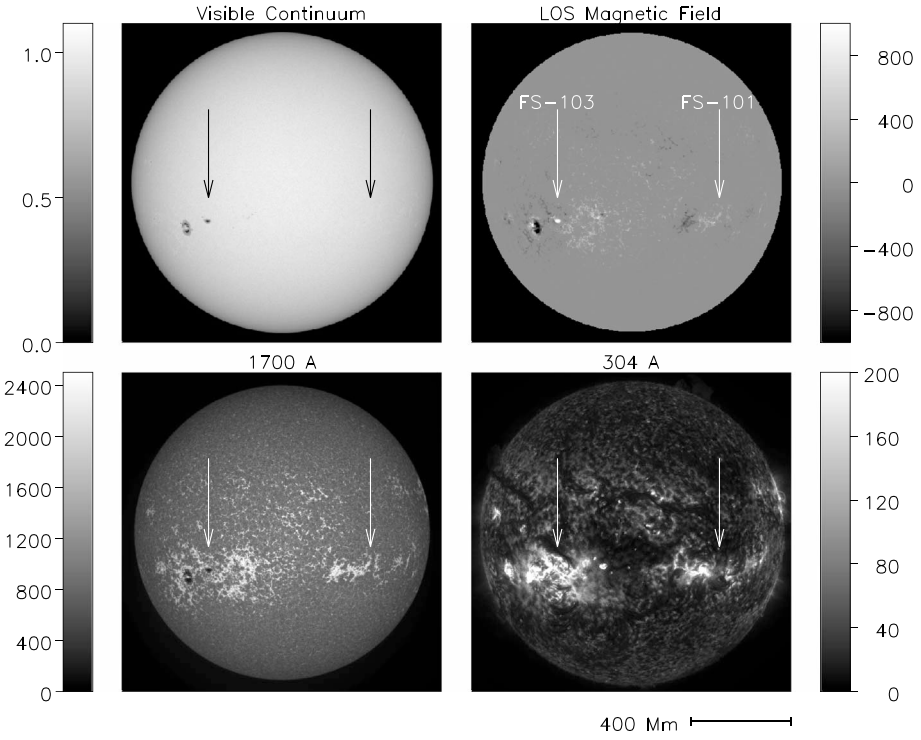

Figure 8. (top left) SDO/HMI visible intensity and (top right) line-of-sight magnetic and (bottom left) AIA intensity maps in 1700 Å and (bottom right) He II 304 Å on 17 November 2014, with both FS-101 and FS-103 (see Figure 7) now in direct view from Earth. At this point, NOAA has designated FS-101 as ARs 12208 (east) and 12207 (west) and, subsequently, FS-103 as ARs 12214 (east), 12209 (middle), and 12213 (west).

at some point for a seismic monitor that is not nearly as sensitive as the observations in electromagnetic radiation against which they are compared (see section 3.2).

To complicate matters, there are instances of seismic signatures whose strengths are similar but whose EUV excess varied by a factor of up to about 3. In fact, very similar disparities characterizes X-ray intensities of active regions in the near hemisphere with similar magnetic fluxes [*Fisher et al.*, 1998; *Falconer et al.*, 1997] and are therefore rather expected of seismic signatures. These disparities appear to have a strong relationship to details of the magnetic configuration, such as magnetic shear across neutral lines [*Falconer et al.*, 1997], which begs not only for the ability to discriminate magnetic polarity to identify neutral lines but also for discrimination of the horizontal component of the magnetic field and its directivity in order to assess its shear. (Note, for example, the strong enhancement of He II 304 Å emission along the major neutral line of the bipolar middle lobe of NOAA AR 11158, comparing Figures 6 (bottom right) and 6 (top right). Extrapolating the heating cited by *Falconer et al.* [1997] from the corona to the transition region would suggest that the heating that gives rise to the strong He II 304 Å emission along this neutral line is contingent upon the degree of magnetic shearing across it.) These are qualities of active regions which seismic signatures by themselves cannot directly discriminate and are the subject of further discussion in the next section.

4.2. Relationship Between Seismic Signatures and Magnetic Flux Distributions

We think we understand the relationship seismic signatures have with magnetic flux distributions better than that which they have with the distributions of excess UV and EUV flux. The former have been modeled with some degree of success [e.g., *Lindsey et al.*, 2010] in terms of the active region photosphere being depressed by magnetic pressure. As discussed in the previous section, the latter depends upon heating of magnetic chromospheres, transition regions and coronae, the physics of which is poorly understood, and whose morphology appears to be more complex, as discussed in the previous section. Like the seismic signatures, the magnetic forces thought to cause Wilson depressions in sunspot umbrae are independent of the sign of the polarity. We think this explains the relative similarity in the morphology of the seismic signature in Figure 6 (top left) to that of the HMI line-of-sight magnetogram in Figure 6 (top right).

Initial efforts to calibrate seismic signatures of active regions with their magnetic fluxes [*González Hernández et al.*, 2007, 2009] showed a positive but poor correlation between the two. Control comparisons between magnetic configurations of active regions before and after farside transit [*González Hernández et al.*, 2007] suggest that this was a result of considerable evolution in magnetic structure in the week or so separating the seismic observations in the far hemisphere and the magnetic observations in the near hemisphere. This has motivated a study that takes advantage of seismic signatures of active regions in the Sun's near hemisphere such as those shown in Figure 6 to clarify this relationship, wherein the magnetic maps are concurrent with the seismic maps. This study is in its beginning stages.

Notwithstanding the quantitative variation in magnetic flux that can take place between an active region's tenure in the far hemisphere and its appearance in the near hemisphere, the recognition of a strong seismic signatures in the far hemisphere is found to be a highly reliable indication of simply the existence of a significant concentration of magnetic flux at its location when it crosses into direct view from Earth [*Liewer et al.*, 2012, 2014], usually one that is subsequently recognized as an active region by NOAA and designated accordingly. Based upon this, the Stanford Farside Seismic Monitor includes a "Large Active Region Discriminator" that recognizes a class of seismic signatures, the approximately 400 strongest signatures during solar activity cycle 24. These signatures are found to anticipate the appearance and location of significant magnetic flux concentrations in the near hemisphere with $(97.5 \pm 0.5)\%$ reliability. Maps and tables of these are posted and archived at http://jsoc.stanford.-edu/data/farside/AR_Maps and http://jsoc.stanford.edu/data/farside-/AR_Lists, respectively.

One aspect of the connection between seismic signatures and magnetic flux distributions is the relationship between strong magnetic regions and the possibility of a flare or CME. From the moment at which an active region appears on the Sun's eastern limb, we typically have several days before the densest component of a CME emanating from the region is likely to hit the Earth. So knowledge of conditions in the far hemisphere is not nearly as urgent from the standpoint of flares and CMEs as it is for forecasting UV and EUV irradiance.

Monitoring of the far hemisphere, however, can apparently be prospectively useful for forecasting the solar wind, including high-speed streams, which emanate from coronal holes. Nick Arge and Carl Henney, at AFRL in Albuquerque, with Gordon McDonald, at New Mexico State University in Las Cruces, are developing

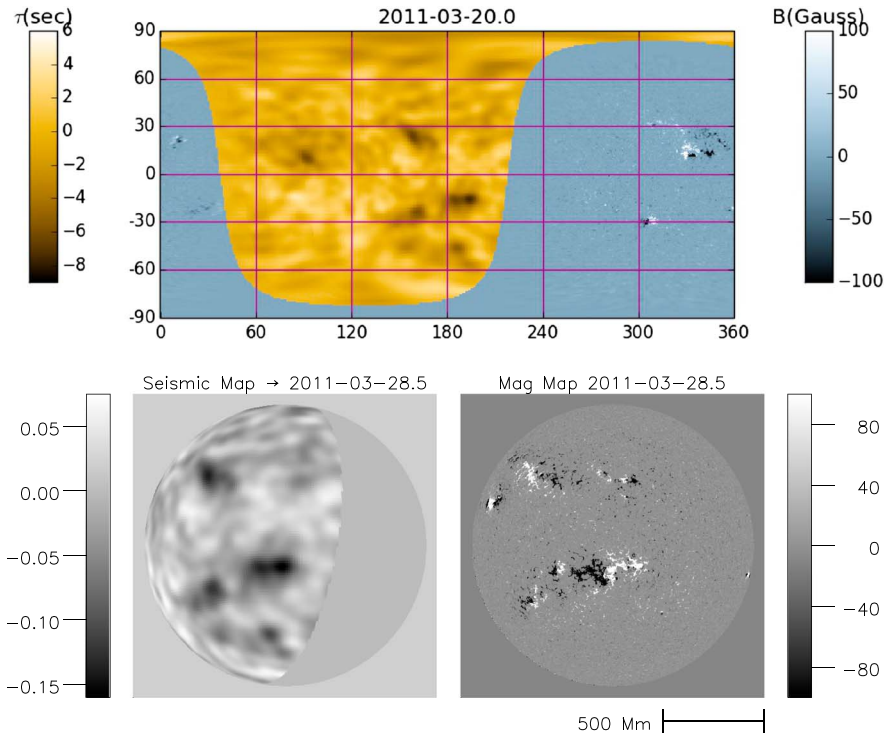

Figure 9. (top) The seismic map shown in longitude-latitude format in the top frame (amber) is projected (bottom left) onto the Sun as viewed from (bottom right) SDO/HMI in a line-of-sight magnetogram 8.5 days later. The seismic signatures are insensitive to the magnetic polarity. However, the Hale polarity law offers a resource whereby this may be guessed with sufficient dependability to give us more realistic models of the coronal magnetic field than are possible without knowledge of a newly emerged seismic signature.

analytical techniques for modeling the coronal magnetic field globally using both nearside and farside maps [see *Arge et al.*, 2013]. The nearside maps show magnetic flux distributions over the near photosphere, including polarity, and their models remember and evolve this distribution appropriately as active regions in the near hemisphere cross into the far hemisphere. The role of the farside signatures is to apprise the modeling algorithm of magnetic flux that is newly emerged in the far hemisphere. The problem for realistic modeling of coronal fields is the need to know the sign of the polarity of the flux. Seismic signatures are insensitive to this (see Figure 6 (top left) and Figure 9 (bottom left)). However, the Hale polarity law offers a promising resource by which this may be guessed with sufficient dependability to give us more realistic models of the coronal magnetic field than would follow from the supposition that there was no significant new magnetic flux where a new strong seismic signature has emerged.

4.3. Direct Space Weather Effects of Activity in the Far Hemisphere

In section 1, we pointed out that near-term impacts of space weather on Earth are predominantly due to magnetic regions in the Sun's near hemisphere, meaning that while the impact of active regions in the far hemisphere could eventually be major, this was not to be expected until they crossed into the near hemisphere—which a large one invariably would, hence its relevance to forecasting. There are, nevertheless, instances of active regions impacting space weather on Earth while still in the far hemisphere to a degree that is significant in some human contexts. CMEs launched from active regions in the Sun's far hemisphere have been known to accelerate protons to high energies and inject them into magnetic streamlines that bring them to Earth [*Dresing et al.*, 2012; *Cohen et al.*, 2014; *Wiedenbeck et al.*, 2013; *Richardson et al.*, 2012]. An especially conspicuous such event was a massive halo CME on 15–16 August 2001, which showered Earth with protons having energies of hundreds of MeV. Figure 10 shows some of the observations we have of this event from SOHO and NOAA's Geostationary Operational Environmental Satellites (GOES; see http://www.polarlicht-vorher-sage.de-/goes_archive). Figure 10c shows a snapshot of the CME by the Large Angle Spectrometric Coronagraph (LASCO) aboard SOHO. Figure 10a plots fluxes of high-energy protons appearing minutes after the top of the CME first cleared the LASCO occulting disk. Figure 10b plots

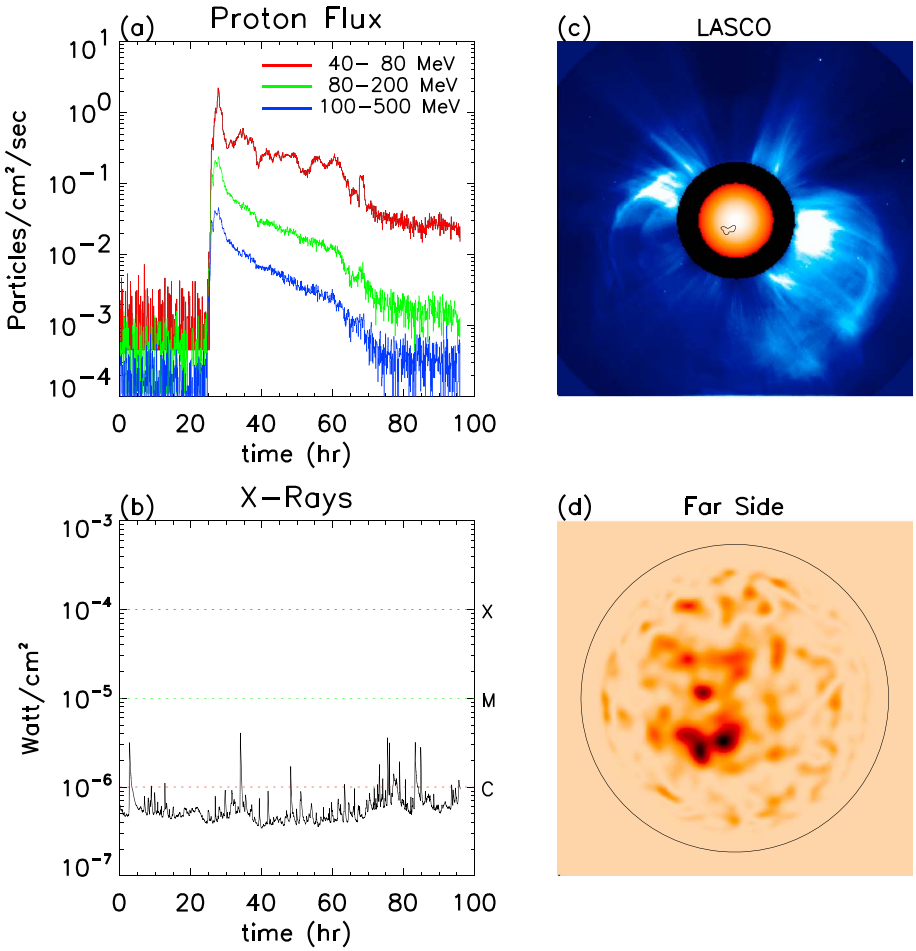

Figure 10. (c) Massive halo CME imaged by the Large Angle Spectrometric Coronagraph (LASCO), aboard the Solar and Heliospheric Observatory (SOHO) at 00:31 UT on 15 August 2001. (a) Fluxes of high-energy protons, which began to arrive minutes after first appearance of the CME to SOHO. (b) Excess X-ray flux from the SOHO vantage is essentially nil, because the CME emanated (we think) from the Sun's far hemisphere; hence, any X-rays from the active region were radiated into the far side of the solar system. (d) A seismic image, presenting the Sun's far hemisphere as viewed directly from SOHO through the near hemisphere, shows the clear signature of an active region at ~0.3 solar radii south (below) and slightly east (left) of disk center. This active region was a composite destined to be designated NOAA 9557 and 9591 about a week later, after it had rotated into direct view from Earth. Reproduced from *Lindsey et al.* [2011], courtesy of InTech (http://www.intechopen.com).

concurrent fluxes of soft X-rays from the Sun. The lack of significant X-ray emission from this event (Figure 10b) is understood to indicate that the CME emanated from the Sun's far hemisphere. The active region from which the CME errupted must in fact have released intense X-rays. However, X-rays travel in straight lines from their sources, and so we understand that these must have been radiated into the far side of the solar system, hence their invisibility from Earth vantage. Because protons are charged particles, their trajectories, in the magnetic environment of the heliosphere, can (indeed, generally do) deviate radically from straight lines emanating from the near neighborhood of the active region from which the CME errupted [*Laitinen et al.*, 2016].

Figure 10d shows the seismic map of the far hemisphere for the 24 h period centered on 15 August 2001 computed from SOHO MDI observations. It shows the signature of a newly emerged active region appearing south (below) and somewhat east (left) of farside disk center, on its way to the Sun's eastern (left) limb from behind. This appears to be the likely source region of the 15 August 2001 CME. NOAA designated this AR 09591 soon after it subsequently crossed the eastern limb and became directly visible from Earth.

In fact, the proton storm from the 15 August 2001 CME happened to be of significant concern to the crew of the International Space Station (ISS), members of which were undertaking an extravehicular activity (EVA)

when it began. Space weather impacts from the far hemisphere such as these, though rare, get to be more than annoying when they show up uninvited during an EVA in Earth orbit. This suggests that planning of EVAs could benefit from a knowledge of exceptionally large active regions even in the Sun's far hemisphere.

5. The Future of Farside Solar Seismology

It should be understood that seismic monitoring of the Sun's far hemisphere is encumbered by stringent technical limitations, familiarly expressed in terms such as "diffraction" and "realization noise," that render it far inferior to electromagnetic imaging in the visible and UV electromagnetic spectra. The signal-to-noise ratio in an image taken by a spaceborne EUV camera in a 1 s exposure exceeds that of an acoustic image integrated for a full day by 2 to 3 orders of magnitude. Nevertheless, the seismic monitors presently mapping the Sun's far hemisphere will reliably detect and identify something approaching 400 active regions transiting the Sun's far hemisphere even in a relatively weak solar cycle. These active regions account for most of the excess UV and EUV emission from the Sun in the years of solar maximum and are usually the ones of predominant concern for space weather forecasting.

For the past several years NASA's twin STEREO spacecraft have been in positions to view the entirety of the far hemisphere from the far side of Earth's orbit about the Sun, making helioseismic mapping of the Sun's far hemisphere unnecessary. After about 2019, STEREO coverage of the Sun's far hemisphere will begin to diminish as these spacecraft drift back to Earth's side of our orbit about the Sun, eventually to become practically nil. And the continuation of STEREO observations in the following decade, when these spacecraft recover their farside vantage, is far from guaranteed.

We are now approaching significant periods during which seismic monitoring will be our only means of detecting and accurately locating newly emerged magnetic flux in the Sun's far hemisphere more than a few hours before it appears on the Sun's eastern limb. The Solar Wind Anisotropies (SWAN) Experiment aboard SOHO can detect the presence of active regions in the Sun's far hemisphere by backscattering of Ly-α radiation from the far side of the solar system. It has not nearly the spatial discrimination of helioseismic diagnostics, but that gives us a good measure of the total EUV brightness emanating from the far hemisphere [*Bertaux et al.*, 2000]. Solar Orbiter, scheduled at this writing to be launched in October of 2018, will orbit the Sun with a period at first of about a year and eventually of about 150 days. It will carry a "Polarimetric and Helioseismic Imager" and have extensive coverage of the Sun's far hemisphere during about half of its orbit for about the succeeding decade. There will be significant periods during which Solar Orbiter and STEREO combined will continue to fully cover the Sun's far hemisphere. There will nevertheless be significant periods in which direct electromagnetic coverage of the Sun's far hemisphere will be next to nil.

On the other hand, Solar Orbiter will be useful for calibrating seismic signatures of active regions in the Sun's far hemisphere made from Earth vantage with concurrently observed magnetic qualities of the same, very much like STEREO that is presently allowing us to do with EUV intensities.

One naturally hopes that human society will eventually develop in such a direction that plain electromagnetic monitoring of the Sun's entire surface — of both near and far hemispheres — will be constantly maintained by spaceborne instruments spread over multiple vantages. This will always tell us much more about solar activity than will ever be possible by just seismic monitoring from near-Earth vantage. The benefits of doing this in a world of billions would already far exceed its expense today. It nevertheless remains attractive to think that seismic monitoring of the Sun's far hemisphere from the near-Earth neighborhood, either from ground-based or spaceborne seismic observatories, will continue for centuries. Seismic monitoring, taking advantage of helioseismic observatories of the future, can be readily available as a backup when other resources fail, and solar observations from Earth or Earth orbit will continue to have a high economy relative to observations from heliocentric orbit. And, necessary or not, seismic monitoring of the Sun's far hemisphere is, plainly speaking, just a terrific load of fun, an ardently stimulating and educational exercise for any student who has reached an age to begin to understand solar activity, solar rotation, how these come together to make space weather what it is for Earth or any other planet, and the role these phenomena have come to play in modern technological civilization during the twentieth century and since. We think that seismic monitoring of the Sun's far hemisphere will enjoy a long future in our relationship with the heliosphere and its crucial role in space weather, and that centuries hence its history in space weather forecasting and research will be looked back upon with distinct pleasure.

Glossary

coherent acoustic egression the wave-mechanical extrapolation, backward in time, of an acoustic field over an observed region of the Sun's surface during a given time period to another surface, from which disturbances that have arrived at the first are supposed to have emanated during a previous time period (cf. coherent acoustic ingression).

coherent acoustic ingression the wave-mechanical extrapolation, forward in time, of an acoustic field over an observed region of the Sun's surface during a given time period to another surface, at which disturbances from the first are expected to arrive during a subsequent time period. The acoustic ingression is a time reverse analogy of the acoustic egression.

p **modes** compression waves with periods of about 5 min that travel through the solar interior. Where the *p* modes impinge into the Sun's surface from below, they cause ripples, called the "solar oscillations."

solar oscillations oscillating ripples on the solar surface caused by *p*-mode waves impinging into it from the underlying solar interior.

Notation

Acronyms

AFRL The Air Force Research Laboratory

AIA The Atmospheric Imaging Assembly, aboard the SDO—which observes the Sun in UV and EUV radiation

CME Coronal mass ejection—massive clouds of gas ejected from the Sun that cause spectacular auroras and other phenomena when they hit Earth

EUV Extreme Ultraviolet—electromagnetic spectrum encompassing wavelengths from 1240 Å down to 100 Å

GOES Geostationary Operational Environmental Satellite, launched and operated by NOAA

GONG The National Solar Observatory's Global Oscillations Network Group, a network of six helioseismic observatories spread around the Earth to maintain constant seismic coverage of the Sun's near surface

HMI The Helioseismic Magnetic Imager—the helioseismic and magnetographic telescope aboard the SDO

ISS The International Space Station

JPL Jet Propulsion Laboratory, operated by NASA—builds satellites

JSOC Stanford's Joint Science Operations Center for the Solar Dynamics Observatory

LASCO Large Angle Spectrometrich Coronagraph, aboard the SOHO spacecraft

MDI Michelson Doppler Imager, an instrument aboard the SOHO spacecraft that monitors solar oscillations

NASA National Aeronautics and Space Administration

NOAA National Oceanic and Atmospheric Administration, Department of Commerce (includes the US Weather Service)

NSO The National Solar Observatory

SDO The spaceborne Solar Dynamics Observatory

SOHO The spaceborne Solar and Heliospheric Observatory

SOI The Solar Oscillations Investigation—project sponsored by NASA and the European Space Agency (ESA) and headquartered at Stanford to develop solar seismology and to model solar thermal and rotational structure

STEREO Twin NASA spacecraft—in heliospheric orbit to observe the Sun from multiple vantages

SWAN Solar Wind ANisotropies instrument, aboard the SOHO spacecraft—observes Ly-α radiation from solar activity backscattered from the interplanetary medium

VSO Virtual Solar Observatory, a solar data analysis center operated by NASA (http://umbra.-nascom.nasa.gov/vso/)

Acknowledgments
Both the science and art of mapping activity in the Sun's far hemisphere owe a great debt to the late Irene González Hernández at the National Solar Observatory's Global Oscillations Network Group (GONG). Irene's hard work was essential in making farside seismology work as a reliable, publicaly accessible synoptic resource. She was equally industrious in opening farside solar seismology to the rapidly growing array of its applications in space weather research and forecasting. We greatly appreciate Phil Scherrer's crucial role in supporting farside solar seismology from its beginning. Phil created the first synoptic website showing seismic maps of the Sun's far hemisphere computed from SOHO/MDI observations and was an enthusiastic and invaluable supporter of the farside seismology effort long before its practicality was realized by most of the solar community at large. We also greatly the role of Frank Hill, Director of GONG, for his crucial role in making it possible to compute seismic maps of the Sun's far hemisphere from ground-based GONG observations, his industry in publishing all available farside maps on the GONG website and making these data products of the Virtual Solar Observatory (VSO), and his work with Tom Wentzel—whom we also thank—on the statistical character of various aspects of seismic images of the Sun's far hemisphere. We most appreciate the hard work by Paulett Liewer, at NASA/JPL, and Jiong Qiu, at Montana State University, to advance our understanding of the relationship between seismic images of active regions and their UV and EUV intensities, taking advantages of concurrent, cospatial observations of the Sun's far hemisphere by NASA's STEREO spacecraft. We appreciate Joe Werne for introducing us to statistical methods that can improve our insight into the relationship between active regions in the Sun's far hemisphere and the seismic signatures they elicit. Finally, we greatly appreciate the insight and constructive comments by the two anonymous reviewers. Work on this chapter was supported by contracts with the National Oceanic and Atmospheric Administration's (NOAA's) Small Business Inovative Research (SBIR) program and the National Aeronautics and Space Administration's (NASA's) Sun-Earth Connection Guest-Investigator Program. The data used to produce Figures 5–9 are made available by Stanford University's Joint Science Operations Center (JSOC) for the Solar Dynamics Observatory (SDO) Project: http://jsoc.stanford.edu. Seismic maps of the Sun's far hemisphere computed from observations by the Helioseismic

References

Arge, C. N., C. J. Henney, I. González Hernández, W. A. Toussaint, J. Koller, and H. C. Godinez (2013), Modeling the corona and solar wind using ADAPT maps that include far-side observations, *Proc. 13th AIP Conf.*, *1539*, 11–14.
Born, M., and E. Wolf (1975a), *Principles of Optics*, pp. 491–505, Pergamon Press, Oxford, U. K.
Born, M., and E. Wolf (1975b), *Ibid.*, 375–378.
Braun, D. C., and A. C. Birch (2008), Surface-focused seismic holography of sunspots: I. Observations, *Solar. Phys*, *251*, 267–289.
Braun, D. C., and C. Lindsey (2000a), Helioseismic holography of active-region subphotospheres, *Sol. Phys.*, *192*, 285–305.
Braun, D. C., and C. Lindsey (2000b), Phase-sensitive holography of solar activity, *Sol. Phys.*, *192*, 307–319.
Braun, D. C., and C. Lindsey (2001), Seismic imaging of the far hemisphere of the Sun, *Astrophys. J. Lett.*, *560*, 189–192.
Braun, D. C., T. J. Duvall Jr., and B. J. LaBonte (1988), The absorption of high-degree p-mode oscillations in and around sunspots, *Astrophys. J.*, *335*, 1015–1025.
Braun, D. C., C. Lindsey, Y. Fan, and S. M. Jefferies (1992), Local acoustic diagnostics of the solar interior, *Astrophys. J.*, *392*, 739–745.
Braun, D. C., C. Lindsey, Y. Fan, and M. Fagan (1998), Helioseismic holography of solar activity, *Astrophys. J.*, *502*, 968–980.
Bertaux, J.-L., E. Quemerais, R. Lallement, E. Lamassoure, W. Schmidt, and E. Kyrölä (2000), Monitoring solar activity on the far side of the sun from sky reflected Lyman α radiation, *Geophys. Res. Lett.*, *27*, 1331–1334.
Cally, P. S. (2000), Modelling p-mode interaction with a spreading sunspot field, *Sol. Phys.*, *192*, 395–401.
Cally, P. S., and T. J. Bogdan (1997), Simulation of f- and p-mode interactions with a stratified magnetic field concentration, *Astrophys. J. Lett.*, *486*, 67–70.
Christensen-Dalsgaard, J., C. R. Proffitt, and M. J. Thompson (1993), A new technique for measuring solar rotation, *Astrophys. J. Lett.*, *403*, 75–78.
Chang, H.-K., D.-Y. Chou, B. J. LaBonte, and the TON Team (1997), Ambient acoustic imaging in helioseismology, *Nature*, *389*, 825–827.
Chou, D.-Y. (2000), Acoustic imaging of solar active regions, *Sol. Phys.*, *192*, 241–259.
Cohen, C. M. S., G. M. Mason, R. A. Mewaldt, and M. E. Wiedenbeck (2014), The longitudinal dependence of heavy-ion composition in the 2013 April 11 solar energetic particle event, *Astrophys. J.*, *793*, 35–44.
Deubner, F.-L. (1975), Observations of low wavenumber nonradial eigenmodes of the Sun, *Astron. Astrophys.*, *44*, 371–375.
Dresing, N., Gómez-Herrero, A. Klassen, B. Heber, Y. Kartavykh, and W. Dröge (2012), The large longitudinal spread of solar energetic particles during the 17 January 2010 Solar Event, *Sol. Phys.*, *281*, 281–300.
Duvall, T. L., Jr., S. D'Silva, S. M. Jefferies, J. W. Harvey, and J. Schou (1996), Downflows under sunspots detected by helioseismic tomography, *Nature*, *379*, 235–237.
Duvall, T. L., Jr., S. M. Jefferies, J. W. Harvey, and M. Pomerantz (1993), Time-distance helioseismology, *Nature*, *362*, 430–432.
Evans, J. W., R. Michard, and R. Servajean (1963), Observational study of macroscopic inhomogeneities in the solar atmosphere. V. Statistical Study of the time variations of solar inhomogeneities, *Astron. Astrophys.*, *26*, 368–382.
Falconer, D. A., R. L. Moore, J. G. Porter, G. A. Gary, and T. Shimizu (1997), Neutral-line magnetic shear and enhanced coronal heating in solar active regions, *Astrophys. J.*, *482*, 519–534.
Fisher, G. H., D. W. Longcope, T. R. Metcalf, and A. A. Pevtsov (1998), Coronal heating in active regions as a function of global magnetic variables, *Astrophys. J.*, *508*, 885–898.
Fontenla, J. M., I. González Hernández, E. Quémerais, and C. Lindsey (2009), *Solar Irradiance Forecast and Far-Side Imaging*, vol. 44, pp. 457–464.
González Hernández, I., F. Hill, and C. Lindsey (2007), Calibration of the far side seismic-holography signature of active regions, *Astrophys. J.*, *669*, 1382–1389.
González Hernández, I., F. Hill, P. H. Scherrer, C. Lindsey, and D. C. Braun (2009), On the success rate of the farside seismic imaging of active regions, *Space Weather*, *8*, S06002, doi:10.1029/2009SW000560.
Hartlep, T., J. Zhao, N. Mansour, and A. G. Kosovichev (2008), Validating time-distance far-side imaging of solar active regions through numerical simulations, *Astrophys. J.*, *689*, 1373–1378.
Ilonidis, S., J. Zhao, and T. Hartlep (2009), Time-distance solar far-side imaging using three-skip acoustic signals, *Sol. Phys.*, *258*, 181–189.
Laitinen, T., A. Kopp, F. Effenberger, S. Dalla, and M. S. Marsh (2016), Solar energetic particle access to distant longitudes through turbulent field-line meanering, *Astron. Astrophys.*, *591*, 18–26.
Leighton, R. B., R. Noyes, and G. W Simon (1962), Velocity fields in the solar atmosphere. Preliminary report, *Astrophys. J.*, *135*, 474–499.
Liewer, P. C., I. González Hernández, J. R. Hall, W. T. Thompson, and A. Misrak (2012), Comparison of far-side STEREO observations of solar activity and active region predictions from GONG, *Sol. Phys.*, *281*, 3–20.
Liewer, P. C., I. González Hernández, J. R. Hall, C. Lindsey, and X. Lin (2014), Testing the reliability of predictions of far-side active regions from helioseismology using STEREO far-side observations of solar activity, *Sol. Phys.*, *289*, 3617–3640.
Lindsey, C., and D. C. Braun (1990), Helioseismic imaging of sunspots at their antipodes, *Sol. Phys.*, *135*, 474–499.
Lindsey, C., and D. C. Braun (1997), Helioseismic holography, *Astrophys. J.*, *485*, 895–903.
Lindsey, C., and D. C. Braun (2000a), Seismic images of the far side of the Sun, *Science*, *287*, 1799–1800.
Lindsey, C., and D. C. Braun (2000b), Basic principles of solar acoustic holography, *Sol. Phys.*, *192*, 261–284.
Lindsey, C., D. C. Braun, S. M. Jefferies, M. F. Woodard, Y. Fan, Y. Gu, and S. Redfield (1996), Doppler acoustic diagnostics of subsurface solar magnetic structure, *Astrophys. J.*, *470*, 636–646.
Lindsey, C., P. S. Cally, and M. Rempel (2010), Seismic discrimination of thermal and magnetic anomalies in sunspot umbrae, *Astrophys. J.*, *719*, 1144–1156.
Lindsey, C., D. C. Braun, I. González Hernández, and A.-C. Donea (2011), Computational Seismic Holography of Acoustic Waves in the Solar Interior, Holography - Different Fields of Application, edited by F. Monroy, pp. 81–106, InTech. [Available from http://www.intechopen.com/books/holography-different-fields-ofapplication/computational-seismic-holography-of-acoustic-wavesin-thesolar-interior.]
Noyes, R., and R. B. Leighton (1963), Velocity fields in the solar atmosphere. II. The oscillatory field, *Astrophys. J.*, *138*, 631–647.
Roddier, F. (1975), Principe de réalisation d'un hologramme acoustique de lo surface du Soleil, *C. R. Acad. Sci. Paris B*, *281*, 93–95.
Rhodes, E. J., R. Ulrich, and G. W. Simon (1977), Observations of nonradial p-mode oscillations on the Sun, *Astrophys. J.*, *218*, 901–919.
Rhodes, E. J., F.-L. Deubner, and R. Ulrich (1979), A new technique for measuring solar rotation, *Astrophys. J.*, *227*, 629–637.
Richardson, I. G., et al. (2012), >25 MeV proton events observed by the high energy telescopes on the TERESO and B Spacecraft andor at Earth during the first ~seven years of the STEREO mission, *Sol. Phys.*, *289*, 3059–3107.
Scherrer, P. H., et al. (1995), The solar oscillations investigation—Michelson Doppler imager, *Solar Phys.*, *162*, 129–188.
Schunker, H., D. C. Braun, C. Lindsey, and P. S. Cally (2008), Physical properties of wave motion in inclined magnetic fields within sunspot penumbrae, *Sol. Phys.*, *251*, 341–359.

Magnetic Imager (HMI) aboard the SDO archived back to 1 May 2011 are archived and made publicly available at http://jsoc.stanford.edu/data/farside, which also posts and archives color composite maps of the Sun's near and far hemispheres.

Skartlien, R. (2001), Imaging of acoustic wave sources inside the Sun, *Astrophys. J.*, *554*, 488–495.
Skartlien, R. (2002), Local helioseismology as an inverse source-inverse scattering problem, *Astrophys. J.*, *565*, 1348–1365.
Spruit, H. C., and T. J. Bogdan (1992), The conversion of p-modes to slow modes and the absorption of acoustic waves by sunspots, *Astrophys. J. Lett.*, *391*, 109–112.
Stein, R. F., T. J. Bogdan, M. Carlsson, V. Hansteen, A. McMurry, C. S. Rosenthal, and A. Nordlund (2004), Theory and simulations of solar atmospheric dynamics, in *Proceedings of the Conference SOHO 13—Waves, Oscillations and Small-Scale Transient Events in the Solar Atmosphere: A Joint View From SOHO and TRACE*, pp. 93–105, European Space Agency, ESA SP-547, Balearic Islands, Spain.
Ulrich, R. (1970), The five-minute oscillations on the solar surface, *Astrophys. J.*, *162*, 993–1002.
van Cittert, P. H. (1939), Kohärenz probleme, *Physica*, *6*, 1129–1138.
Wang, Y.-M., and N. R. Sheeley (1994), The rotation of photospheric magnetic fields: A random walk transport model, *Astrophys. J.*, *430*, 399–412.
Wang, Y.-M., N. R. Sheeley, and A. G. Nash (1991), A new solar cycle model including meridional circulation, *Astrophys. J.*, *383*, 431–442.
Wiedenbeck, M. E., G. M. Mason, C. M. S. Cohen, N. V. Notta, R. Gómez-Herrero, and D. K. Haggerty (2013), Observations of solar energetic particles from ^{3}He-rich events over a wide range of heliographic longitude, *Astrophys. J.*, *762*, 54–62.
Zernike, F. (1938), The concept of degree of coherence and its application to optical problems, *Physica*, *5*, 785–795.